BIOMATERIALS FOR THE CENTRAL NERVOUS SYSTEM

Contract No. NO1-NS-1-2338

Quarterly Progress Report #16

October 31, 2005

The University of Michigan and
The University of Utah

David C. Martin and Patrick A. Tresco

Quarterly Progress to:	National Institute of Health
Contract Monitor:	Joseph Pancrazio, Ph.D.
Research Contract	"Biomaterials for the Central Nervous System"
Contract No.	NO1-NS-1-2338
Principal Investigators:	David C. Martin and Patrick A. Tresco
Date:	October 31, 2005

Overview

This report is a summary of our activity in the fifteenth quarter of our contract, corresponding to the period from July 31, 2005 to October 31, 2005. We discuss the electrochemical polymerization of PEDOT in a hydrogel network, and present TEM images of the alginate network both before and after polymerization. We also provide some details about the impedance and charge capacity of nanotubular conducting polymer films deposited on neural prosthetic electrodes. We compare these data with equivalent circuit models and find that a parallel model fits better than a series model.

The Tresco group also describes their most recent work to evaluate the biological response of various coatings implanted in the CNS.

INTRODUCTION

PEDOT and polypyrrole, both inherently conductive polymers, have been deposited on the gold electrode sites of CNCT intracortical neural probes in order to reduce the impedance of the electrode for improved unit detection and recording, and to increase the charge delivery capacity of the electrode coatings for higher stimulation currents without producing irreversible electrochemical processes or tissue damage (Cui 2001a,b, 2003a,b; Xiao 2004a,b; Yang 2004a,b, 2005). Conformal hydrogel electrode coatings have been used as a mechanical barrier between the stiff silicon probe and the brain tissue in order to limit the incapacitating immune response to probe micromotion and to the foreign body itself. By combining the conformal hydrogel coatings with conductive polymer networks extending from individual electrode sites it is possible to recover the neuronal signals lost by the thin hydrogel coating (Kim. 2004). In previous quarterly reports we described the methods necessary for electrochemical deposition of the conductive polymer poly(3,4-ethylene dioxythiophene) (PEDOT) around living cells and in tissue. We also characterized the electrical properties, morphology of the films, as well as the health and viability of cells that had been polymerized. Recently we have determined that cells can be encapsulated in the conductive polymer-hydrogel coatings to direct tissue integration and healing of the coated probe. We have now investigated the electrical properties of these electrode coatings as well as the morphological details of the incorporation of PEDOT into the hydrogels using transmission electron microscopy.

METHODS

Hydrogel scaffolds: Alginate powder (high G, med viscosity. FMC biopolymer) was dissolved in phosphate-buffered saline (PBS) at a concentration of 2 % (w/v). Hydrogels were crosslinked by dropping 20ul of alginate into a solution of 4 % (w/v) CaCl2 in Hank's Balanced Salt Solution (HBSS) for 5 minutes. Crosslinked beads were kept in HBSS in a humidified incubator at 37°C and 5% CO2.

SY5Y Human Neuroblastoma cells: Cells were cultured in a humid incubator at 37°C and 5% CO2 in media consisting of Dulbecco's modified Eagle's medium (DMEM) (Invitrogen) supplemented with 10% Fetal Bovine Serum (FBS) and 1% antibiotic-antimicotic. 1ml of SY5Y HNBs at concentrations of 10^5, 5 x 10^5, and 10^6 cells/ml were mixed with 1 ml of 2 % (w/v) alginate and vortexed until mixed.

Polymerization of PEDOT: An insulated gold microwire was inserted into SY5Y alginate beads. Electrochemical deposition from the monomer solution (0.01M EDOT (Bayer AG)) with and without poly(styrene sulphonate) (PSS) in phosphate-buffered saline (PBS)) was accomplished using an AutoLab PGStat12 (EcoChemie, Netherlands) potentiostat/galvanostat in a three electrode setup. Deposition currents and duration were varied to study effects on polymer formation and cell viability.

Electron Microscopy: Samples for transmission electron microscopy were first fixed in 2.5 % Glutaraldehyde in PBS overnight. Samples were then washed in Sorenson's buffer in a cacodylate buffer and then stained with Ruthenium Red, Uranyl Acetate, Osmium Tetrachloride overnight. TEM samples are then dehydrated slowly in graded ethanol washes and then mounted

in graded epoxy steps. Ultramicrotomed samples (70 nm) were mounted on copper TEM grids and observed in the Philips CM-100 TEM at the Morphology and Image Analysis Core at UM.

Electrical Characterization: Electrochemical Impedance Spectroscopy (EIS) was performed using an AutoLab Potentiostat/Galvanostat PGStat 12 (EcoChimie, Netherlands) on the cell-seeded PEDOT-hydrogel coatings to determine capacitive and resistive behavior of uncoated versus coated electrodes across many frequencies (1 – 1 MHz). Cyclic voltammetry (CV) was used to investigate the charge transfer capacity of SY5Y-PEDOT-hydrogel electrode coatings. The microelectrode was swept through a potential of -1.0 to 1.0 V at a scan rate of 100 mV/s.

RESULTS

Electrochemical impedance sprectroscopy of alginate hydrogels cells shows increased impedance across all frequencies >10 Hz when SY5Y cells are incorporated before PEDOT deposition (Figure 1). A comparison of the impedance at 1 kHz, the frequency associated with detecting neural activity, shows impedance decrease of 1-2 orders of magnitude after PEDOT is added to the hydrogel-cell network (Figure 2). Decreased impedance corresponds to increased sensitivity, signal strength, and reduced thermal noise.

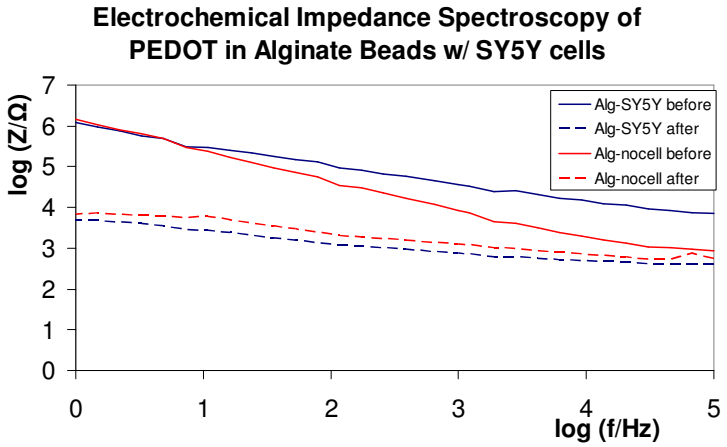

Figure 1. Electrochemical Impedance Spectroscopy of SY5Y-seeded alginate hydrogels before and after PEDOT deposition.

Cyclic Voltammetry (CV) was used to determine the charge capacity of the electrodes before and after modification and their usefulness in stimulating neuronal depolarization and activation. The charge capacity, proportional to the area within the CV curve, of Au-SS microwire in alginate with and without cells was between 10-50 µC (Figure 3). The electrochemical deposition of PEDOT in the cell-seeded hydrogel resulted in a diffuse electrode network within the hydrogel with increased charge capacitance. The charge capacity of a metallic electrode in alginate hydrogel without cells increased 30x after PEDOT was deposited from the electrode site. For SY5Y-seeded hydrogels, the charge capacity increased by over 2640x.

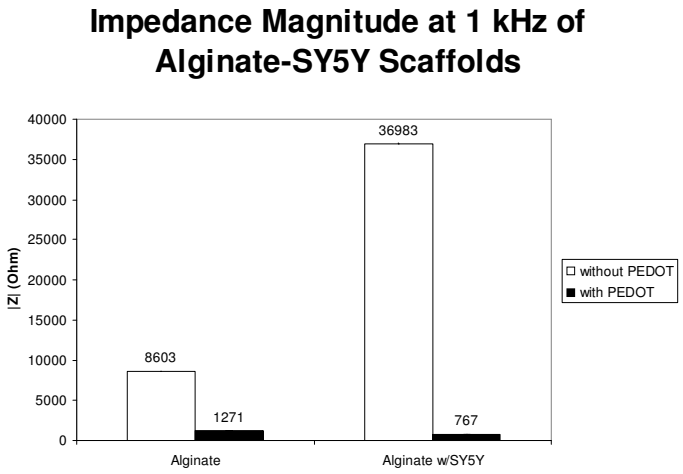

Figure 2. Impedance at 1 kHz of SY5Y-seeded alginate hydrogels before and after PEDOT deposition shows the dramatic decrease in impedance due to PEDOT.

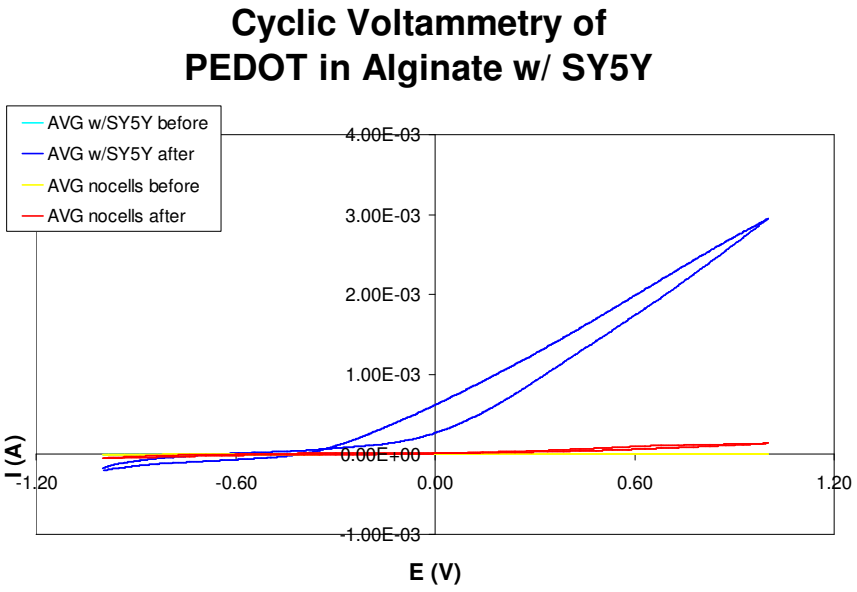

Figure 3. Cyclic Voltammetry of SY5Y-seeded hydrogels before and after PEDOT deposition. The area enclosed by the curve is proportional to amount of charge that can be stored and delivered from the electrode. PEDOT deposition increases the charge delivery capacity by over 2640x when cells were present.

Transmission electron microscopy of the cell-seeded alginate networks reveals that the PEDOT is grown around the alginate network fibers as opposed to within the pores of the hydrogel (Figure 4). The networks themselves are composed of thin filaments corresponding to bundles of alginate chains. The filaments are linked together into a network structure having an average pore size of around 200 nm. After PEDOT polymerization, the structure is similar, but the filaments are noticeably denser and thicker. The average fiber diameter for alginate fibers without PEDOT is 5.12 ± 1.2 nm while the fibers grow to 7.45 ± 1.8 nm when PEDOT is deposited. The results suggest that the PEDOT deposits around the alginate scaffold without causing a significant rearrangement of the crosslinked chains. Presumably this structure is stabilized because the efficiency of growing PEDOT along the alginate network is much more efficient than growing outward in the thickness direction. The result is an open network that should maintain facile mass transport through the gel.

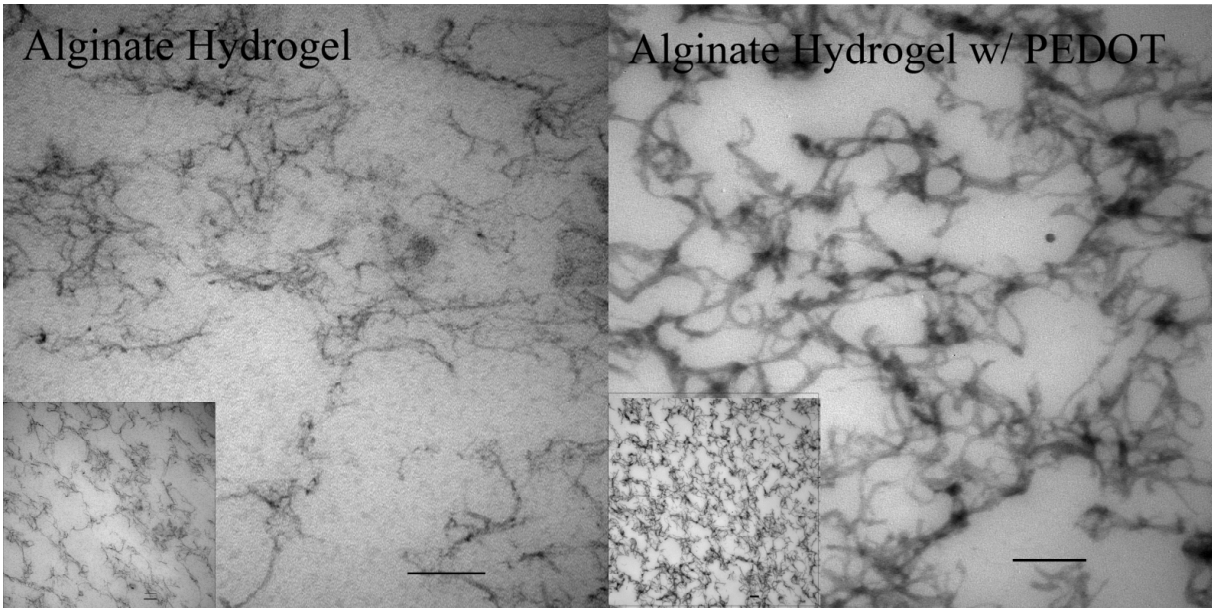

Figure 4. Transmission electron micrographs of unmodified alginate hydrogels (left) and with PEDOT conductive polymer deposited within the network (right). Scale bar is 100 nm. Insets are lower magnification views showing the overall uniformity of the microstructure.

CONCLUSIONS

Conductive polymers deposited into hydrogel scaffolds can be used to create electrode coatings with low impedance and high charge delivery capacity while retaining the high porosity of the hydrogel. These PEDOT-hydrogel coatings can also be used to deliver cells to the site of electrode implantation in order to promote biointegration of the probe with nervous tissue. Studies are underway to study the effects of cell delivery and communication *in vitro* and *in vivo*.

REFERENCES

Cui XY, et al.. (2001a) J Biomed Mater Res. 56(2):261-72.
Cui XY, et al. (2001b). SENSORS AND ACTUATORS A-PHYSICAL 93 (1): 8-18.
Cui XY, et al. (2003a). Biomaterials. 24(5):777-87.
Cui XY, Martin DC. (2003b) SENSORS AND ACTUATORS A-PHYSICAL 103 (3): 384-394.
Kim DH, et al.. J Biomed Mater Res. 2004 Dec 15;71A(4):577-85.
Xiao, Y., et al. (2004a). Sensors and Actuators B: Chemical, 99(2-3), 437-43.
Xiao, Y., et al. (2004b). Journal of Electroanalytical Chemistry, 573, 43-48.
Yang, J., & Martin, D. C. (2004a). Sensors and Actuators A:Physical, 113(2), 204-11.
Yang, J., & Martin, D. C. (2004b). Sensors and Actuators B: Chemical, 101(1-2), 133-42.
Yang, J. et al.(2005). Acta Biomaterialia, 1(1), 124-136.

Electrical properties and surface morphology of conducting polymer films and nanotubes for surface modification of neural microelectrode arrays

The electrode--host interface is a significant problem affecting the long-term use of neural prosthetics in vivo. The engineering of bioactive electrode coatings has been investigated for its potential to promote in-growth of neural tissue, reduce shear stress, and enhance signal transport from electrons to ions at the electrode-host interface. As we have reported in previous progress reports, we have found that films of electrospun nanofibers can be deposited on the surface of these devices, followed by electrochemical polymerization of conducting polymers such as polypyrrole (PPy) and poly(3,4-ethylenedioxythiophene) (PEDOT). After polymerization, the nanofibers can be dissolved, leaving tiny channels and pores in the conducting polymer that facilitate efficient signal transport and communication with the neural tissue The electrical properties of the functionalized probes were examined with impedance spectroscopy, cyclic voltammetry and the structure examined by optical and electron microscopy. We also calculated electrical properties of electrolyte-coating-electrode interface using equivalent circuit modeling.

Materials & methods

Poly (L-lactide) (PLLA, RESOMER® L 210) with inherent viscosity 3.3-4.3 dl/g was purchased from Boehringer Ingelheim Pharma GmbH & Co. (KG, Germany). Poly (lactide-co-glycolide) PLGA 75/25 with inherent viscosity was prepared from Alkermes Inc. Dexamethasone (M.W. = 392.5 g/mol) was purchased from Alexis Corporation. 3, 4-ethylenedioxythiophene (EDOT, BAYTRON® M) with molecular weight 142.17 g/mol was received from H.C. Starck Inc. (Newton, MA). Phosphate buffer saline (PBS, pH= 7.4) was purchased from Mediatech Inc.

Fabrication of electrospun nanofiber templates

PLLA nanofibers and PLLA nanofibers loaded with dexamethasone were prepared by electrospinning. PLLA solution was prepared by dissolving 0.72 g PLLA in 10 ml of chloroform at a temperature of 50 ºC for 10 hr in order to have a homogenous solution with PLLA concentration of 4% (w/v). PLLA nanofibers were directly deposited on the 10 microfabricated electrode arrays by electrospinning. The electrospinning process was carried out in an electrical field of 0.6 kV/cm with flow rate of 0.25 ml/h for 1 min. The neural probes were held at a distance of 11 cm from syringe needle.

Electrochemical deposition of conducting polymers

The electrochemical process was performed for acute and chronic probes on each electrode site by an Autolab PGSTAT 12 (EcoChemie, Utrecht, Netherlands) in galvanostatic mode with a conventional four-electrode configuration at room temperature. EDOT monomer (21.4 µl) was added to 10 ml of PBS and stirred at room temperature to make EDOT concentration of 0.02 M. The solution was purged with nitrogen gas for 20 min. The working and sensing electrodes were connected to electrode site. The reference and counter electrode were connected to a platinum wire within the EDOT/PBS solution. EDOT was polymerized on each electrode sites and around the PLLA and PLLA loaded dexamethasone nanofibers at a

current density of 0.9 mA/cm^2 for 30 min. After electrochemical deposition was completed, the PLLA core fibers were removed by soaking the probe tips in dichloromethane for 10 min.

Electrochemical Impedance Spectroscopy (EIS)

An Autolab PGSTAT 12 and Frequency Response Analyzer (FRA) software were used to record impedance spectra of electrode sites for 10 neural probes. A solution of 0.1 M phosphate buffer solution (PBS, pH = 7) was used as an electrolyte in a four-electrode cell. The working electrode was connected to electrode site through a connector. The counter electrode was connected to a platinum foil that was placed in a glass container. An Ag/AgCl reference electrode and the neural microelectrode tip were immersed in glass container of electrolyte. An AC sinusoidal signal of 5 mV in amplitude was used to record the impedance over a frequency range of 1-10^5 Hz.

Cyclic Voltammetry (CV)

CV was performed for 10 neural probes using an Autolab 12 instrument in a four-electrode configuration as described earlier. A scan rate of 100 mV/s was used, and the potential on the working electrode was swept between −0.9 to 0.5 V. Before each CV curve was recorded, several cycles were swept to insure that the film had reached a stable state. The data was captured by GPES software.

Results

Impedance spectroscopy (EIS) showed that the impedance of electrode site decreased significantly by using conducting polymers and that PEDOT was more effective than PPy. However, nanotubular structures of conducting polymers could improve electrical properties of electrode site. We observed that impedance of electrode site changed from 800 kΩ for bare gold to 100 kΩ by coating with film of PPy, 30 kΩ by coating with Ppy nanotubes, 20 kΩ by coating with PEDOT, and 4 kΩ by coating with PEDOT nanotubes at 1 KHz (Fig. 2A). Figure 1 shows SEM images of electrode sites after modification with conducting polymer films and nanotubes. Cyclic voltammetry (CV) revealed that charge transfer capacity density was increased significantly by using conducting polymer nanotubes. As shown in Figure 2C the PEDOT nanotubes showed the highest value for charge transfer capacity density (0.37 C/cm^2).

We have found that the impedance of the neural microelectrodes can be significantly decreased (by about 2 orders of magnitude) (Fig. 2A) and the charge transfer capacity significantly increased (by about 3 orders of magnitude) (Fig. 2B) by creating conducting polymer nanotubes on the electrode surface.

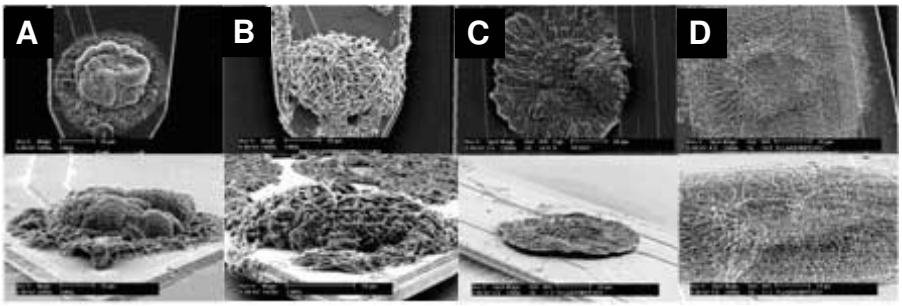

Figure 2. Scanning electron microscopy (SEM) images of top and 3D view of conducting polymer films and nanotubes on the electrode sites: (A) PPy film, (B) PPy nanotubes, (C) PEDOT film, and (D) PEDOT nanotubes.

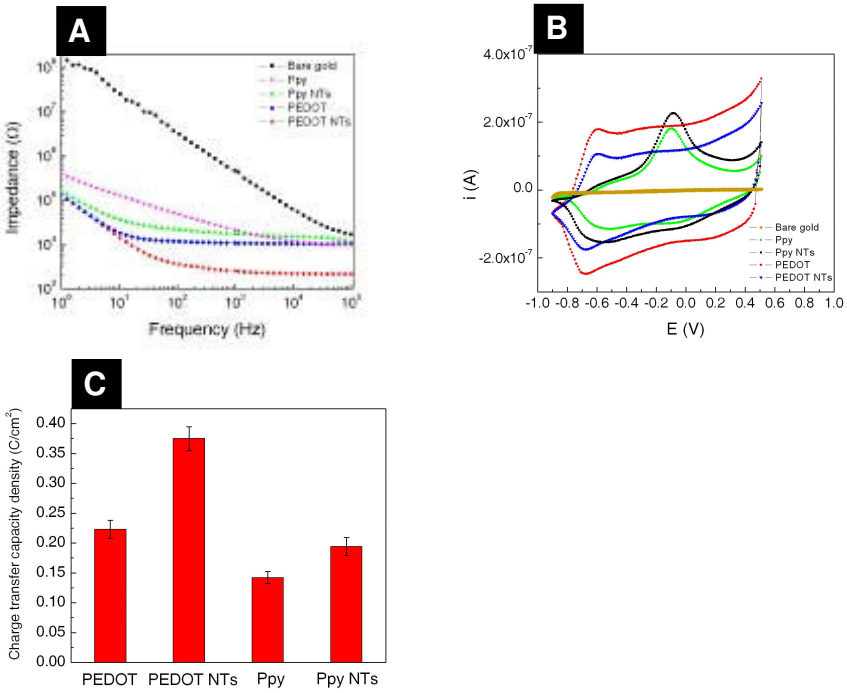

Figure 3. Electrical properties of conducting polymer films and nanotubes on the electrode sites: (A) impedance spectroscopy, (B) cyclic voltammetry, and (C) charge transfer capacity

We also created equivalent circuit models in order to analyze and better predict the electrical properties of coating based on their composition and microstructure. The circuit elements are: solution resistance (Rs), coating capacitance (Cc), coating resistance (Rc), double layer capacitance (Cdl), charge transfer resistance (Rt), and diffusion impedance (T). We used ZSimpWin ver. 3.2 software for data analysis and equivalent circuit simulations. We used two equivalent circuit models in order to model the solution-electrode-coating interface. In the first model coating elements were assumed to be in series with electrode-solution interface elements (Fig. 3a) and in the second model the coating elements were assumed to be in parallel with electrode-solution interface elements (Fig. 3b).

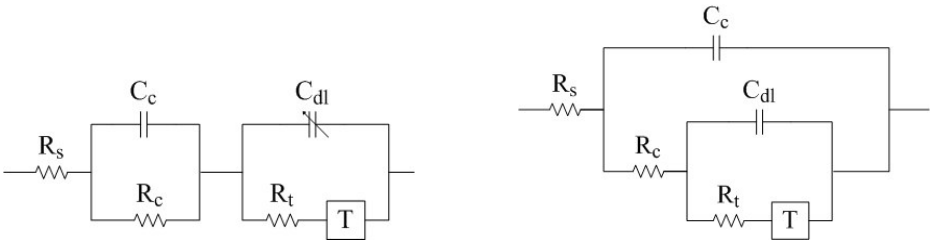

Figure 4. Equivalent circuit modeling of electrolyte-conducting polymer-electrode interface (A) Coating elements are series with electrode-electrolyte interface and (B) coating elements are parallel with electrode-electrolyte interface. Solution resistance (Rs), coating capacitance (Cc), coating resistance (Rc), double layer capacitance (Cdl), charge transfer resistance (Rt), and diffusion impedance (T).

The **T** circuit element is characteristic of a film that contains a fixed amount of electroactive substance. The classical "thin layer electrochemistry" cell is an example of such a system. Batteries or supercapacitors also may share this behavior. The common feature is the fixed amount of electroactive material present. Once it has been consumed, it can not be replenished.

Equations for the T element

The equations for the complex admittance ($\mathbf{Y}(\omega)$) and complex impedance ($\mathbf{Z}(\omega)$) are given by the equations below. The **T** circuit element gets its name from the hyperbolic tangent (tanh) admittance response.

$$\vec{\mathbf{z}}(\omega) = \left\{ \frac{1}{Y_0 \sqrt{j\omega}} \right\} \coth\left[B\sqrt{j\omega} \right] \qquad \vec{\mathbf{Y}}(\omega) = \left\{ Y_0 \sqrt{j\omega} \right\} \tanh\left[B\sqrt{j\omega} \right]$$

If the thickness of the thin layer is δ, then the constant B is related to this thickness and the diffusion coefficient, D. The parameter B characterizes the time it take for a reactant to diffuse from one side of the layer to the other.

$$B = \delta / \sqrt{D}$$

We fit the measured impedance and phase angle to equivalent circuit models using ZWinSimp software. Figures 5 and 6 shows the measured impedances and phase angles as well as calculated impedance and phase angle from cure fitting data for polypyrrole (PPy), polypyrrole nanotubes (PPy NTs), PEDOT, and PEDOT nanotubes (PEDOT NTs). The value of calculated circuit elements is shown in Table 1. As it has been demonstrated in the table the parallel circuit elements have lower values of the chi-squared error function, indicating a better fit of these models to the experimental data.

Table 1. Equivalent circuit model parameters

	Rs(CcRc)(Cdl(RtT)) Series				Rs(Cc(Rc(Cdl(RtT)))) Parallel			
	Ppy	Ppy NTs	PEDOT	PEDOT NTs	Ppy	Ppy NTs	PEDOT	PEDOT NTs
Rs (Ω)	9764	4018	1.04E4	6416	9764	1.132E4	9244	6849
Cc (F)	4.798E-8	1.43E-10	1.198E-6	1.213E-6	1.917E-9	7.207E-10	1.827E-9	4.221E-9
Rc (Ω)	5757	1.073E4	1.085E7	3.043E7	1711	5150	1307	689.7
Cdl (F)	5.222E-7	1.214E-6	6.968E-6	0.0001107	5.825E-7	1.215E-6	4.086E-7	6.181E-7
n	0.5323	0.5915	0.6154	0.1567	0.5399	0.6745	0.932	0.9421
Rt (Ω)	0.1131	5170	1998	2747	1.069E5	8144	101.7	140.4
T (Ω)	4.566E-7	3.264E-6	0.000192	4.945E-5	4.346E-7	2.714E-6	1.066E-5	5.084E-6
B	0.4505	0.1405	0.8243	0.005782	0.3819	0.1303	0.07795	0.1257
Chi-Square	3.165e-03	8.624e-04	3.294e-04	1.063e-04	1.928e-04	8.275e-04	6.142e-05	1.170e-05

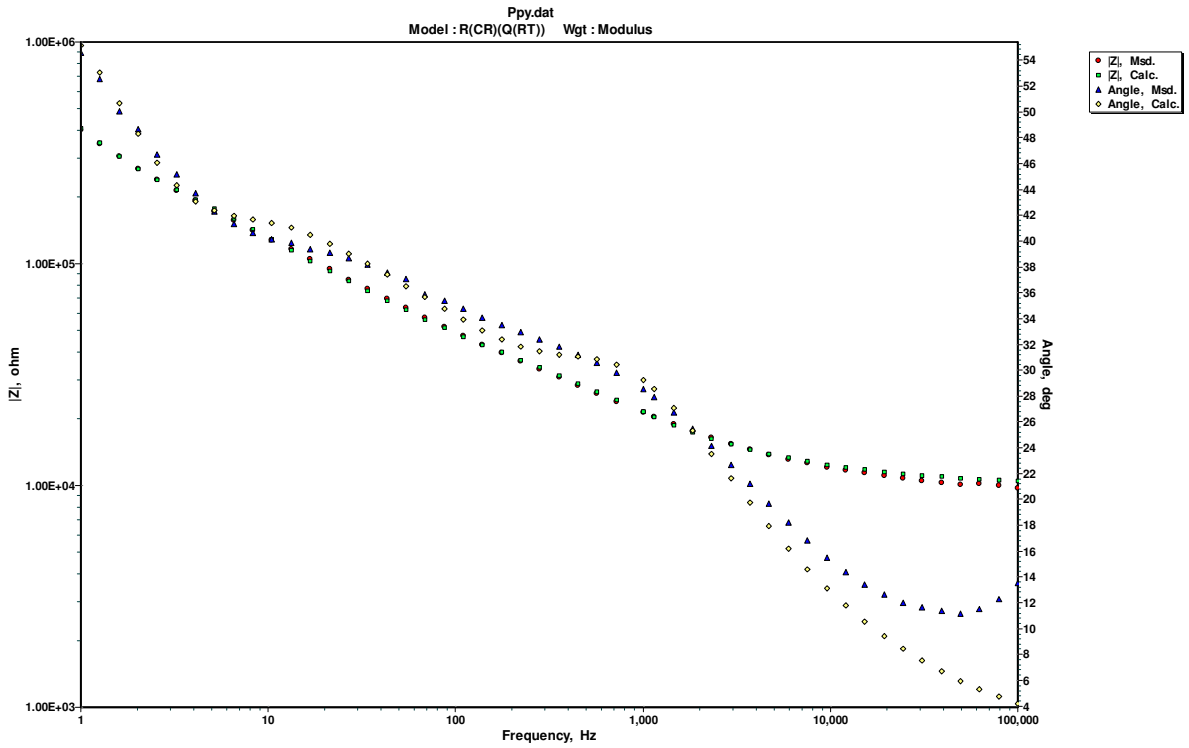
Ppy.dat
Model : R(CR)(Q(RT)) Wgt : Modulus
|Z|, Msd.
|Z|, Calc.
Angle, Msd.
Angle, Calc.
|Z|, ohm
Angle, deg
Frequency, Hz
1.00E+06
1.00E+05
1.00E+04
1.00E+03
1
10
100
1,000
10,000
100,000

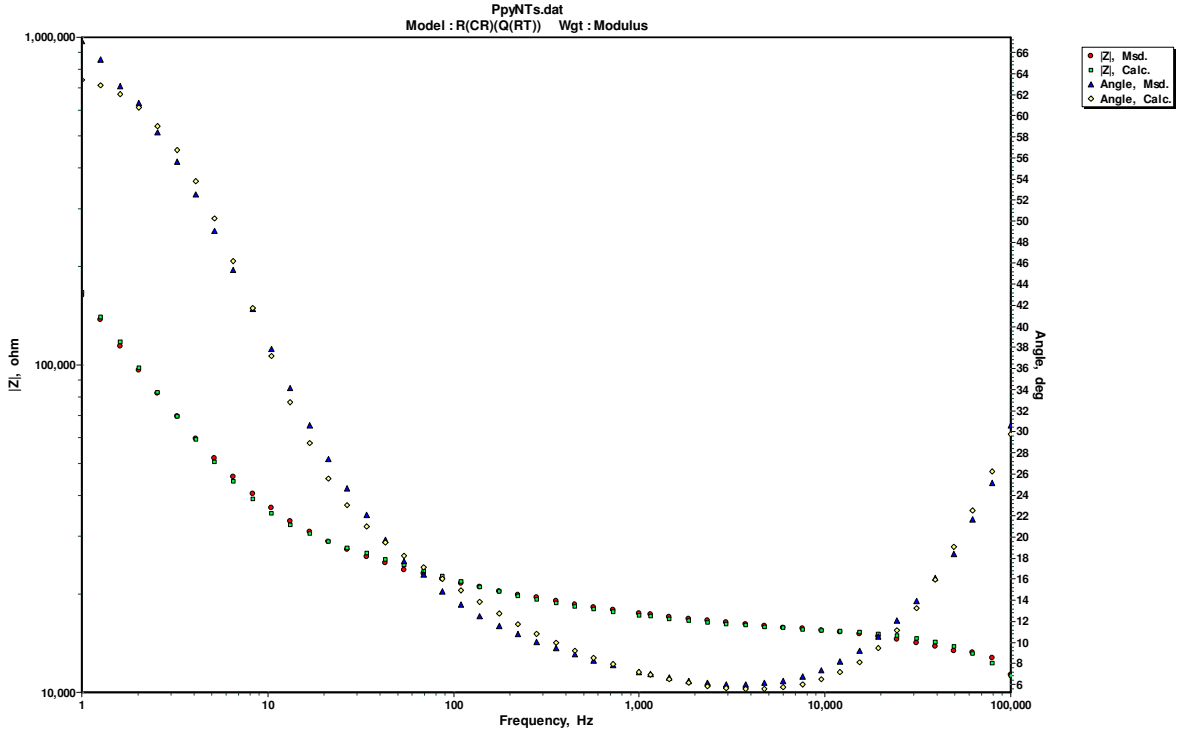
PpyNTs.dat
Model : R(CR)(Q(RT)) Wgt : Modulus
|Z|, Msd.
|Z|, Calc.
Angle, Msd.
Angle, Calc.
|Z|, ohm
Angle, deg
Frequency, Hz
1,000,000
100,000
10,000
1
10
100
1,000
10,000
100,000

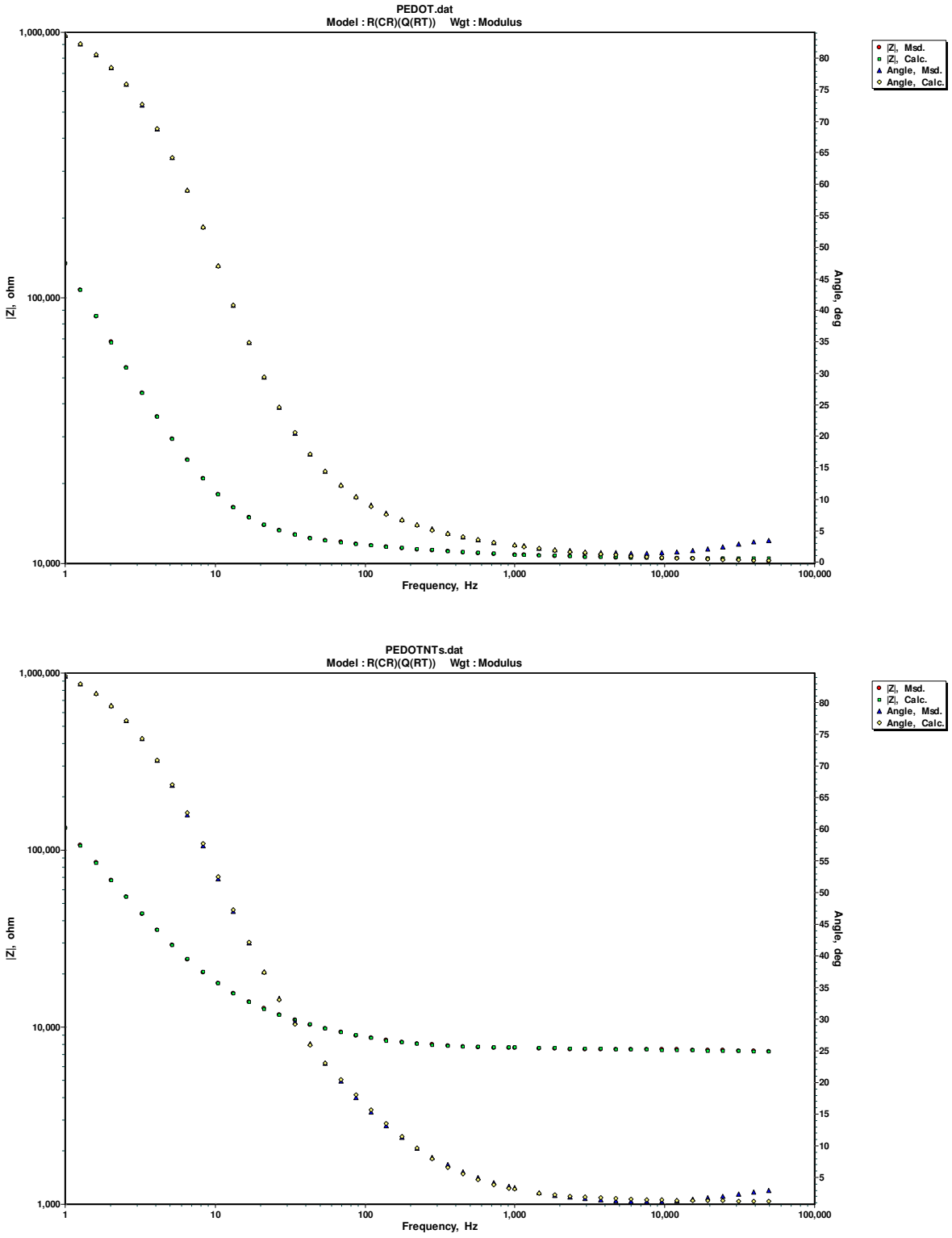

Figure 4. Impedance and phase angles graphs of series circuit model Rs(CcRc)(Cdl(RtT)) for polypyrrole, polypyrrole nanotubes, PEDOT, and PEDOT nanotubes.

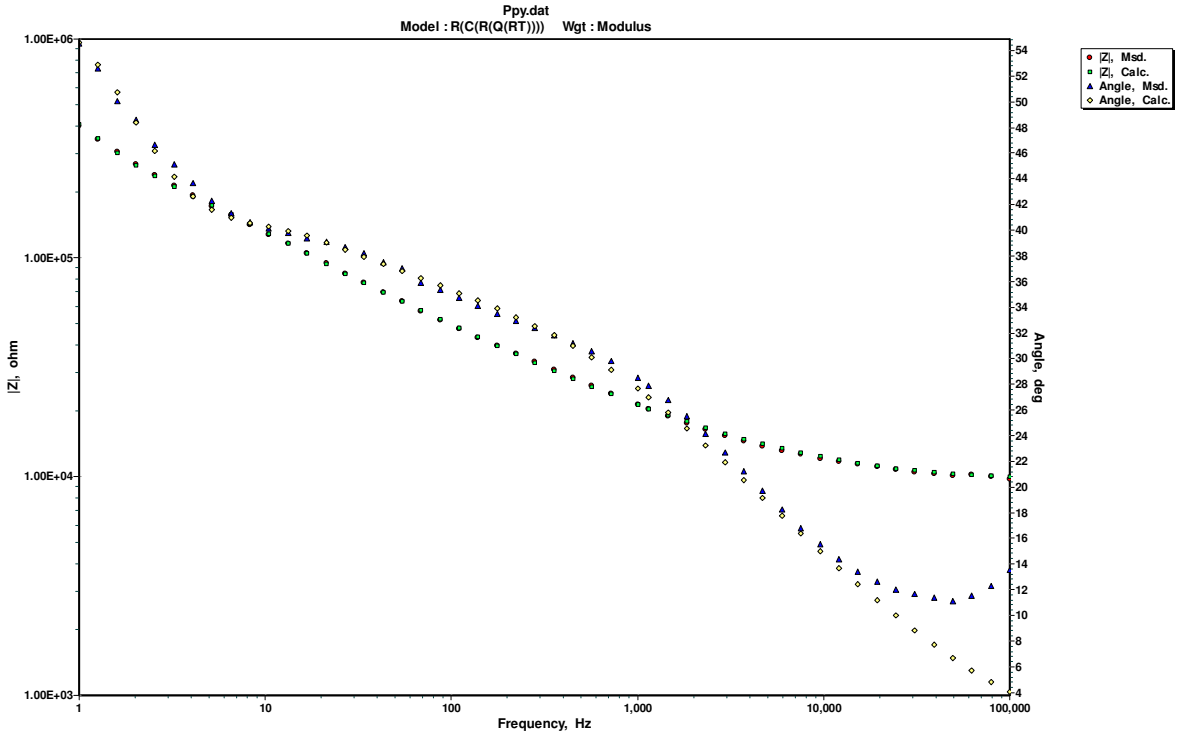
Ppy.dat
Model : R(C(R(Q(RT)))) Wgt : Modulus
|Z|, Msd.
|Z|, Calc.
Angle, Msd.
Angle, Calc.
|Z|, ohm
Angle, deg
Frequency, Hz
1.00E+06
1.00E+05
1.00E+04
1.00E+03
1
10
100
1,000
10,000
100,000

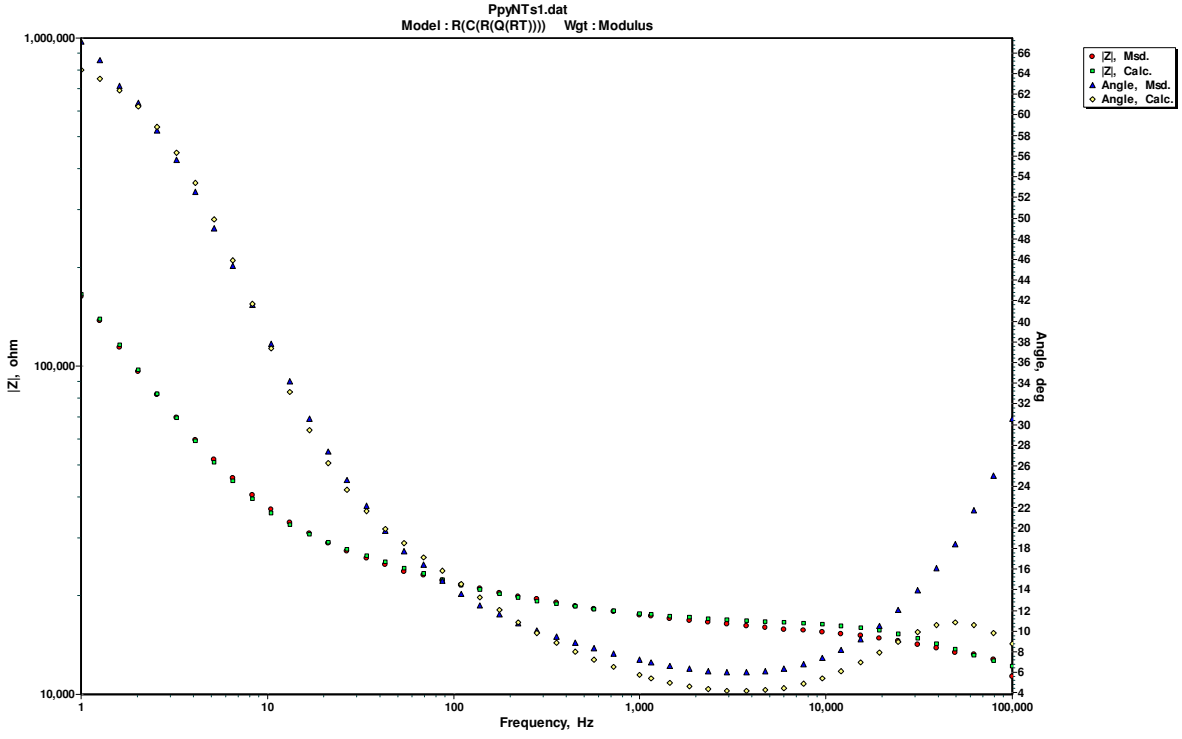
PpyNTs1.dat
Model : R(C(R(Q(RT)))) Wgt : Modulus
|Z|, Msd.
|Z|, Calc.
Angle, Msd.
Angle, Calc.
|Z|, ohm
Angle, deg
Frequency, Hz
1,000,000
100,000
10,000
1
10
100
1,000
10,000
100,000

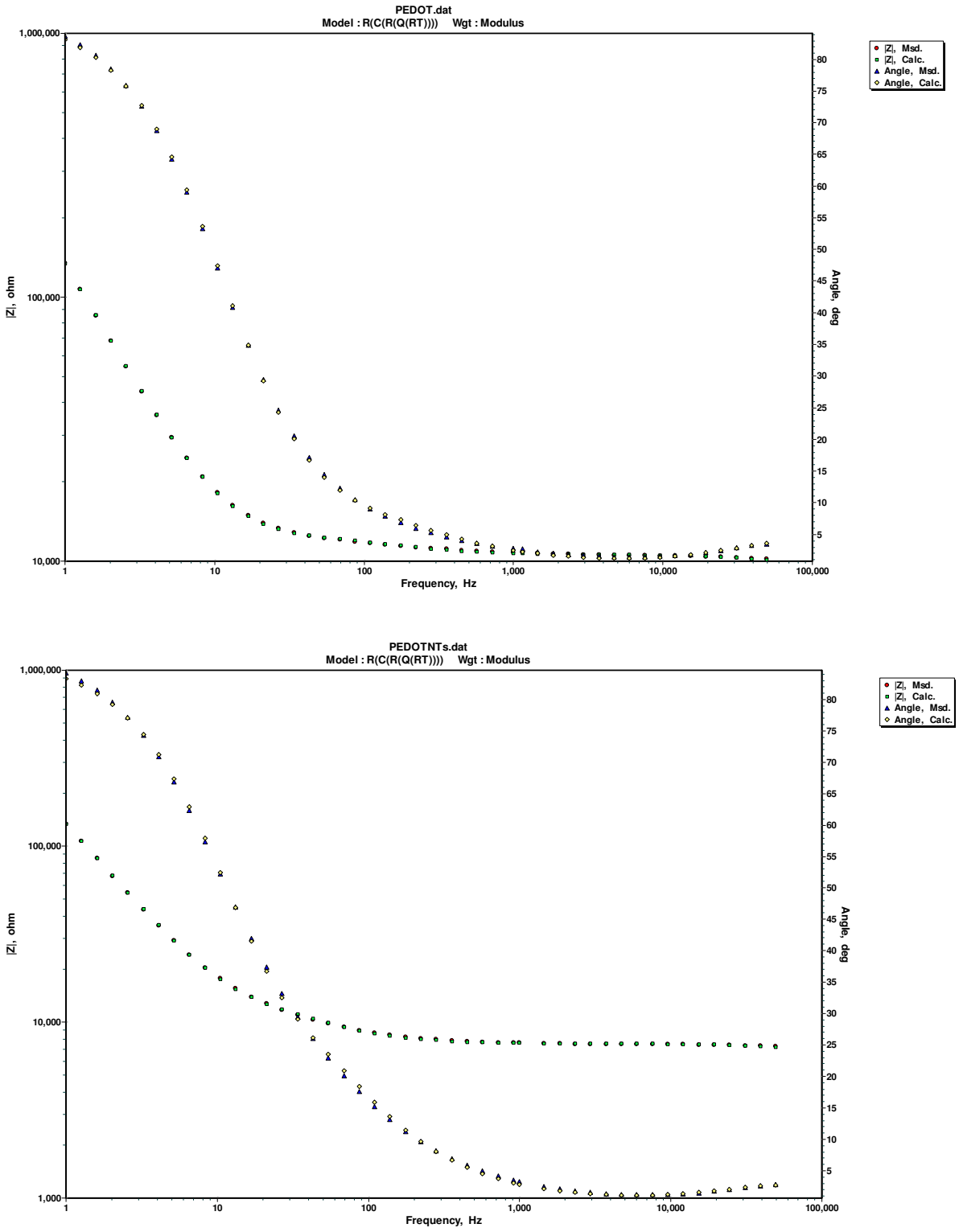

Figure 5. Impedance and phase angles graphs of series circuit model Rs(Cc(Rc(Cdl(RtT)))) for polypyrrole, polypyrrole NTs, PEDOT, and PEDOT nanotubes.